INTERFACE

rsif.royalsocietypublishing.org

Research

Cite this article: Yeo GC, Kondyurin A, Kosobrodova E, Weiss AS, Bilek MMM. 2017 A sterilizable, biocompatible, tropoelastin surface coating immobilized by energetic ion activation. *J. R. Soc. Interface* **14**: 20160837. http://dx.doi.org/10.1098/rsif.2016.0837

Received: 18 October 2016
Accepted: 10 January 2017

Subject Category:
Life Sciences–Physics interface

Subject Areas:
biomimetics, biophysics

Keywords:
biomimetic material, plasma ion implantation, polyethersulfone, tropoelastin, ethylene oxide, sterilization

Authors for correspondence:
Giselle C. Yeo
e-mail: giselle.yeo@sydney.edu.au
Alexey Kondyurin
e-mail: kond@mailcity.com

Electronic supplementary material is available online at https://dx.doi.org/10.6084/m9.figshare.c.3675919.

THE ROYAL SOCIETY PUBLISHING

A sterilizable, biocompatible, tropoelastin surface coating immobilized by energetic ion activation

Giselle C. Yeo[1,2,3], Alexey Kondyurin[1], Elena Kosobrodova[1], Anthony S. Weiss[2,3,4] and Marcela M. M. Bilek[1]

[1]School of Physics, [2]Charles Perkins Centre, [3]School of Life and Environmental Sciences, and [4]Bosch Institute, University of Sydney, Sydney, New South Wales 2006, Australia

GCY, 0000-0001-6071-8899

Biomimetic materials which integrate with surrounding tissues and regulate new tissue formation are attractive for tissue engineering and regenerative medicine. Plasma immersion ion-implanted (PIII) polyethersulfone (PES) provides an excellent platform for the irreversible immobilization of bioactive proteins and peptides. PIII treatment significantly improves PES wettability and results in the formation of acidic groups on the PES surface, with the highest concentration observed at 40–80 s of PIII treatment. The elastomeric protein tropoelastin can be stably adhered to PIII-treated PES in a cell-interactive conformation by tailoring the pH and salt levels of the protein–surface association conditions. Tropoelastin-coated PIII-treated PES surfaces are resistant to molecular fouling, and actively promote high levels of fibroblast adhesion and proliferation while maintaining cell morphology. Tropoelastin, unlike other extracellular matrix proteins such as fibronectin, uniquely retains full bioactivity even after medical-grade ethylene oxide sterilization. This dual approach of PIII treatment and tropoelastin cloaking allows for the stable, robust functionalization of clinically used polymer materials for directed cellular interactions.

1. Introduction

Synthetic polymers such as polyethersulfone (PES) are commonly used in the production of tissue-contacting medical devices, artificial organs and blood purification articles [1]. PES has excellent physico-chemical properties, including high glass transition temperature and chemical resistance as well as relatively low flammability, water absorption and dielectric loss. However, in a biological environment, PES is prone to the non-specific protein adsorption that triggers adverse host reactions [2,3]. Coating of a polymer surface by functional biomolecules not only protects the surface from non-specific molecular adhesion, but also actively elicits a desired biological outcome.

Biomimetic surface coatings using extracellular matrix (ECM) proteins have been used to emulate the natural cell environment, to improve cell adhesion and proliferation, and to stimulate specific cellular responses and direct new tissue formation. A particularly stable and functionally versatile ECM component is tropoelastin, the precursor of elastin, which confers mechanical strength and resilience to elastic tissues such as skin, lungs and blood vessels [4]. Through interactions with multiple cell receptors such as integrins [5], glycosaminoglycans [6] and the elastin binding protein [7], tropoelastin can modulate the adhesion, proliferation and activity of a range of cell types, including fibroblasts [8], endothelial cells [9], smooth muscle cells [10] and chondrocytes [6]. Another unique property of tropoelastin is its inherent resistance to sterilization processes such as steam autoclaving and gamma irradiation [11], a necessary step for devices in clinical use.

Plasma immersion ion implantation (PIII)-treated polymers provide an excellent platform for the irreversible immobilization of functional

biomolecules, including proteins such as tropoelastin [9]. PIII treatment significantly improves polymer wettability [12], thereby reducing denaturation of adsorbed proteins. The high concentration of radicals produced by PIII treatment in the polymer surface layer results in a significant increase of the polar component of surface free energy [12]. Although hydrophobic recovery is observed after PIII treatment, the water contact angles of PIII-treated polymers typically do not reach the values measured before the treatment [13,14]. The high concentration of surface radicals as detected by electron spin resonance (ESR) spectroscopy persists for months after PIII treatment [15,16]. These radicals enable rapid, direct covalent binding between the polymer surface and biomolecules without the need for chemical linkers [17]. The irreversible binding of target biomolecules eliminates exchange with subsequent proteins. Furthermore, proteins form a denser layer on the PIII-treated polymer surface compared with pristine polymers [18,19], thereby further reducing the opportunity for non-specific protein adhesion.

The functionality of immobilized proteins such as tropoelastin critically depends on their conformation on the material surface [9]. The extent and manner of protein adsorption on a synthetic surface are strongly influenced by surface chemical properties, wettability, roughness and charge [20,21], as well as the pH, ionic strength, temperature and concentration of the protein solution during surface association [22]. In this paper, we investigated the effect of PIII treatment on the chemical structure and wettability of PES. We tested the capability of PIII-treated PES for covalent tropoelastin binding and explored the influence of protein–surface association pH on the stability and functionality of the immobilized tropoelastin, and its resistance to ethylene oxide (EtO) sterilization. Finally, we tested the ability of PIII-treated, tropoelastin-functionalized PES to promote cell attachment and proliferation and maintain cell morphology in comparison with bare PES, using human dermal fibroblasts as a model cell type.

2. Methods and materials

PES films with a density of 1.37 g cm^{-3}, tensile strength of 70–95 MPa and a coefficient of thermal expansion of 55×10^{-6} K^{-1} were purchased from Goodfellow Cambridge Ltd (Huntingdon, UK). Samples for ESR studies were 6×6 cm with a thickness of 0.025 mm. Samples for all other experiments were 0.25 mm thick, and cut to 1.5×1.5 cm for Fourier transform infrared attenuated total reflectance (FTIR-ATR) spectroscopy and transmittance measurements, 1×1 cm for X-ray photoelectron spectroscopy (XPS), 1×5 cm for wettability measurements and 0.8×0.6 cm for all biological experiments.

Recombinant wild-type human tropoelastin without domain 26A, corresponding to residues 27–724 of GenBank entry AAC98394, was obtained from Elastagen (Sydney, Australia). GM3348 human dermal fibroblasts were obtained from Coriell Cell Repositories (NJ, USA). All other biological reagents were purchased from Sigma Aldrich, unless otherwise specified.

2.1. Plasma immersion ion implant treatment

Inductively coupled radiofrequency (RF) nitrogen plasma powered at 13.56 MHz was used as a source for PIII. The base pressure of the vacuum system was 10^{-5} Torr (10^{-3} Pa), and the pressure of nitrogen during the implantation was 2×10^{-3} Torr (0.267 Pa). The forward power was 100 W with reverse power of 12 W when matched.

The samples were placed on a stainless steel holder with a mesh made of the same material. The mesh was electrically connected to the holder and held in front of the sample parallel to its surface. The distance between the sample and the mesh was 5 cm. Plasma ions were accelerated by the application of high voltage (20 kV) bias pulses of 20 µs duration at a frequency of 50 Hz and drawing a current of 1.2 mA to the substrate holder and its mesh. The samples were treated for 40–800 s corresponding to ion implantation fluences of 5×10^{14}–10^{16} ions cm^{-2} and stored in air at room temperature. Because oxidation of PIII-treated surfaces reaches saturation 5–7 days after treatment, samples were analysed at least one week after PIII treatment to allow the surface chemistry to stabilize.

2.2. Transmittance measurements

The transmission spectra of untreated and PIII-treated PES were measured using a Cary 5E UV–Vis–NIR spectrophotometer in the wavelength range of 300–700 nm.

2.3. Electron spin resonance spectroscopy

The concentration of unpaired spins in untreated and 800 s PIII-treated PES (a month after PIII treatment) was investigated using an ESR spectrometer, Bruker Elexsys E500, operating in X band with a microwave frequency of 9.35 GHz and a central magnetic field of 3330 G at 20°C. The spectrometer was calibrated using a weak pitch sample with KCl. To estimate the concentration of the unpaired spins in the PES samples, a strong pitch sample with α,α′-diphenyl-β-picrylhydrazyl and spin concentration of 10^{16} spins cm^{-3} was used. The ESR spectra of empty tubes were also recorded.

2.4. Fourier transform infrared attenuated total reflectance spectroscopy

To characterize the surface chemistry of untreated and PIII-treated PES, FTIR-ATR spectra from untreated and 40–800 s PIII-treated samples without protein coating were measured using a Digilab FTS7000 FTIR spectrometer fitted with a multibouncing ATR accessory (Harrick, USA) with a trapezium germanium crystal at an incidence angle of 45°. PES films with a 1.5×1.5 cm area were placed to fully cover the 1 cm width of the ATR crystal. Good optical contact was indicated by high absorbance values (1–2 units) of the most intense spectral peaks. To obtain sufficient signal-to-noise ratio and resolution of spectral bands, 500 scans were taken at a resolution of 4 cm^{-1}. The spectra were measured a month after PIII treatment.

2.5. X-ray photoelectron spectroscopy

Chemical composition of untreated and 800s PIII-treated PES (a month after PIII treatment) was also analysed using XPS (Specs, Germany) equipped with Al X-ray source with monochromator operating at 200 W, a hemispherical analyser and a line delay detector with nine channels. Survey spectra were acquired for binding energies in the range from 0 to 1200 eV using 30 eV pass energy. C 1s, O 1s and N 1s region spectra were acquired at a pass energy of 23 eV with 10 scans to

obtain high spectral resolution and low noise level. The spectra in S 2s and S 2p region were acquired at a pass energy of 30 eV with 50 scans and 0.5 s dwelling time to minimize noise level. The peaks were fitted with a sum of Gauss (70%) and Lorentz (30%) functions using Marquardt–Levenberg fitting procedure of CasaXPS. The peaks were quantified using relative sensitivity factors supplied by the spectrometer manufacturer. Linear background was subtracted, and the spectra were charge corrected by setting the C 1s C–C/H component to 285.0 eV.

2.6. Contact angle measurements

The contact angles between a PES surface and two liquids (de-ionized water and diiodomethane) were measured using a Kruss DS10 contact angle analyser employing the sessile drop method. The contact angles were measured two weeks after PIII treatment. The surface free energy and its polar and dispersive components were calculated using the Owens–Wendt–Rabel–Kaelble model.

2.7. Tropoelastin coating of surfaces

Tropoelastin immobilization on plasma and PIII-treated PES was performed a week after treatment. PES samples were soaked in 20 $\mu g\ ml^{-1}$ tropoelastin dissolved in PBS (10 mM phosphate, 150 mM NaCl, pH 7.4) or in PB (10 mM phosphate, pH 11.5) at 4°C overnight, then washed with PBS to remove excess unbound protein.

2.8. Fibronectin coating of surfaces

Fibronectin coating on PIII-treated PES was performed a week after treatment. PES samples were incubated in 2 $\mu g\ ml^{-1}$ fibronectin from human plasma (Sigma Aldrich) dissolved in PBS at 4°C overnight. Samples were washed with PBS then stored in PBS at 4°C or air dried until use as indicated.

2.9. Enzyme-linked immunosorbent assay detection of tropoelastin

Where indicated, tropoelastin-coated PES samples were washed with 5% (w/v) sodium dodecylsulfate (SDS) at 80°C for 10 min and rinsed with PBS. Samples were then blocked with 3% (w/v) bovine serum albumin (BSA) for 1 h at room temperature and washed with PBS. Surface-bound tropoelastin was detected with 1 : 2000 dilution of mouse anti-elastin BA4 antibody for 1 h and 1 : 5000 dilution of goat anti-mouse IgG conjugated with horseradish peroxidase for 1 h. The tropoelastin C-terminus was detected with 1 : 5000 dilution of anti-C-terminal peptide antibody (Biomatik) for 1 h and 1 : 5000 dilution of goat anti-rabbit IgG conjugated with horseradish peroxidase for 1 h. Bound antibody was visualized with substrate solution (1.04 $mg\ ml^{-1}$ 2,2′-azino-bis(3-ethylbenzothiazoline-6-sulfonic acid) diammonium salt, 0.05% (v/v) H_2O_2, 10 mM CH_3COONa, 5 mM Na_2HPO_4) at 37°C for 1 h. Sample absorbance at 405 nm was read with a plate reader.

2.10. Cell attachment

Untreated and PIII-treated PES with and without tropoelastin were blocked for 1 h at room temperature with 10 $mg\ ml^{-1}$ BSA that had been heat-denatured at 80°C for 10 min and then cooled on ice. GM3348 human dermal fibroblasts were trypsinized with 0.25% trypsin–EDTA at 37°C for 3 min, centrifuged at 800*g* for 5 min and resuspended in serum-free Dulbecco's minimal Eagle medium (DMEM). Samples were washed with PBS and seeded with 1.5×10^5 cells cm^{-2} at 37°C in 5% CO_2 for 1 h. Non-adherent cells were washed off with PBS, whereas adherent cells were fixed with 3% (w/v) formaldehyde in PBS for 20 min. Excess fixative was removed with PBS, and the fixed cells were stained with 0.1% (w/v) crystal violet in 0.2 M MES buffer, pH 5.0 at room temperature for 1 h. Samples were rinsed thoroughly in reverse osmosis water prior to solubilizing the stain with 10% (w/v) acetic acid. Absorbance was measured at 570 nm using a plate reader. Absorbance readings from standards containing 20%, 40%, 60%, 80% and 100% of the seeding density were fitted to a linear regression, which was used to convert sample absorbance into percentage of cell attachment.

2.11. Ethylene oxide sterilization

Untreated and PIII-treated PES with and without protein were air dried at room temperature for 2 days, placed in uncovered multi-well plates and EtO sterilized by the Sterilizing Services at Randwick Hospitals Campus (NSW, Australia). Samples were exposed to EtO for 1 h at 56°C and aerated for approximately 19 h at 56°C. To determine the effect of sterilization on tropoelastin retention and activity, unsterilized controls were prepared at the same time as sterilized samples but were left dry at room temperature until analysis.

2.12. Cell imaging

Bright-field microscope images of human dermal fibroblasts cultured on bare or tropoelastin-coated, BSA-blocked untreated and PIII-treated PES were taken at 1 and 7 days post-seeding.

2.13. Cell proliferation

EtO-sterilized untreated and PIII-treated PES samples with and without tropoelastin were BSA-blocked similarly to a cell attachment assay and seeded with human dermal fibroblasts at a density of 1.0×10^4 cells cm^{-2} in DMEM with 10% fetal bovine serum. The culture medium was changed every 2 days. At 1, 3, 5 and 7 days post-seeding, samples were washed with PBS, and the bound cells were fixed and stained as described in the cell attachment assay.

2.14. Statistical analyses

Results were expressed as mean $\pm$ s.e. ($n = 3$, unless otherwise indicated). Two-way analysis of variance (ANOVA) tests were used to determine statistical significance, denoted in the figures as ($^*p < 0.05$), ($^{**}p < 0.005$) or ($^{***}p < 0.001$).

3. Results

3.1. Transmittance

Transmittance of PIII-treated PES decreases with increasing PIII treatment time (figure 1*a*) owing to the formation of carbonized clusters in the modified surface layer [23]. PES colour changes from a light brown colour with 40 s of PIII treatment to a darker brown with 800 s of treatment.

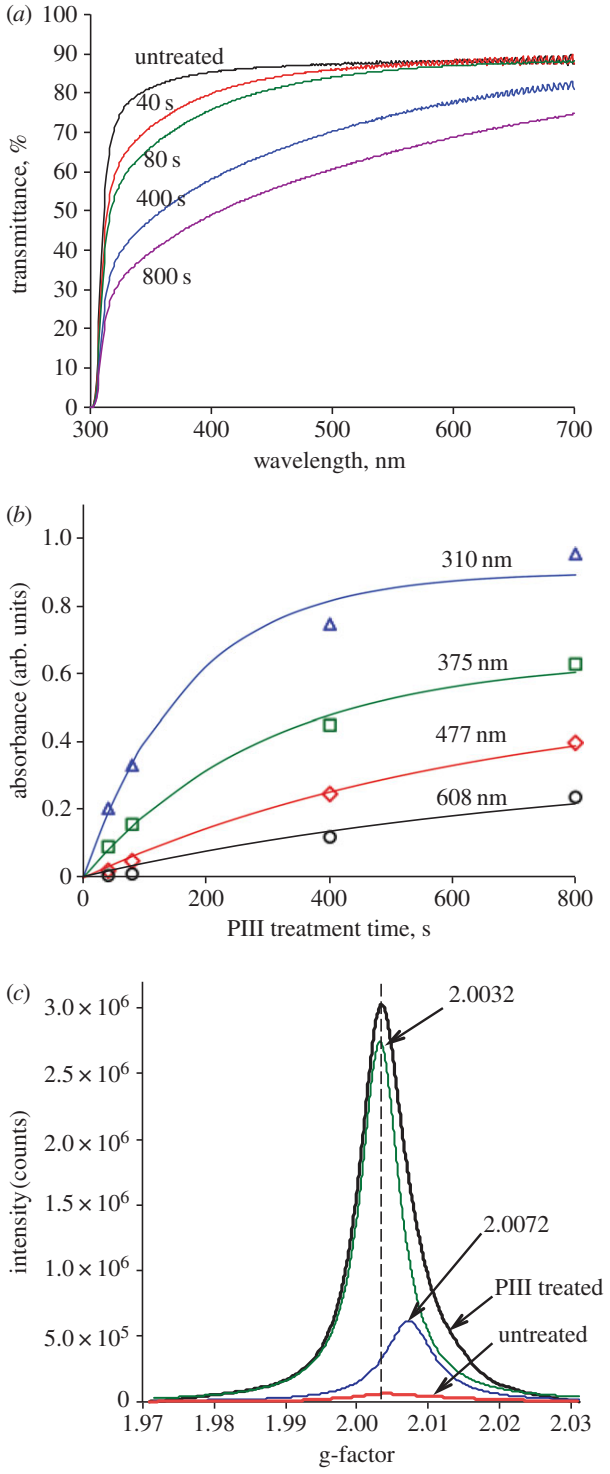

Figure 1. (*a*) Transmittance of untreated and PIII-treated PES. PIII treatment time was 40, 80, 400 and 800 s. (*b*) The difference between the absorbance of untreated and PIII-treated PES at 310, 375, 477 and 608 nm as a function of PIII treatment time. Data were fitted to $A(t) = a(1 - \exp(-t/k))$. (*c*) ESR spectra of untreated and 800 s PIII-treated PES. The peak of 800 s PIII-treated PES was fitted with a sum of two Lorenz functions with positions of peak maximums at g-factors of 2.0032 and 2.0072. The ESR spectrum of 800 s PIII-treated PES was measured a month after the treatment.

Quantitative analysis of the carbonization was performed using UV–visible transmission spectra. The absorbance at 310, 375, 477 and 608 nm (figure 1*b*) corresponds to naphthalene-like, antracene, naphthacene [24] and quaterrylene (eleven conjugated aromatic rings) [25] structures, respectively. To obtain the rate constants of the formation of these structures, the curves shown in figure 1*b* were fitted using the following equation:

$$A(t) = a\left(1-\exp\left(\frac{-t}{k}\right)\right), \tag{3.1}$$

where A is absorbance at fixed wavelength, t is PIII treatment time, a is absorbance at $t = \infty$ and k is rate constant. The fitting parameters are shown in electronic supplementary material, table S1. The rate constants of the formation of naphthalene-like structures, antracene, naphthacene and quaterrylene are found to be 170, 300, 650 and 800 s, respectively.

3.2. Electron spin resonance spectroscopy

Figure 1*c* shows ESR spectra of untreated and 800 s PIII-treated PES. Untreated PES contains a low concentration of unpaired electrons that can be generated by environmental factors such as light, heat, cosmic rays and oxygen species (ozone, peroxide and excited oxygen molecules), as well as trapped residual radicals remaining after the polymerization process. The ESR peak of 800 s PIII-treated PES is asymmetric. This peak was fitted using a sum of two Lorenz functions with the positions of the peak maximums at g-factors of 2.0032 and 2.0072 corresponding to carbon and sulfur radicals, respectively.

According to SRIM simulations [26], the depth of penetration of 20 keV nitrogen ions in PES is about 74 nm. The most radicals produced by PIII treatment are concentrated in this layer and they contribute predominantly to ESR intensity. In untreated PES, the ESR intensity corresponds to the radicals within the entire PES film whose thickness was 0.25 mm. Consequently, the real difference between the ESR intensity of untreated and 800 s PIII-treated PES is about 500 times higher than that shown in figure 1*c*.

3.3. Fourier transform infrared attenuated total reflectance spectroscopy

FTIR-ATR spectrum of untreated PES has characteristic vibration lines corresponding to C–H (2900–3200 cm^{-1}), C–O (1150 cm^{-1}) and S–C (1105 cm^{-1}) groups (figure 2*a*).

PIII treatment results in the carbonization and post-treatment oxidation of the PES surface. FTIR-ATR spectra of PIII-treated PES contain vibration lines corresponding to O–H (3700–2700 cm^{-1}), C=O (1750–1650 cm^{-1}) and aromatic C=C (1610 cm^{-1}) groups. The asymmetric shape of the O–H peak indicates the presence of acidic groups. The concentration of the acidic groups has a maximum at 40–80 s of PIII treatment (figure 2*b*). The concentration of C=O and C=C groups increases with increasing PIII treatment time and reaches saturation after 400 s of PIII treatment.

3.4. X-ray photoelectron spectroscopy

XPS of untreated PES contains C 1s, O 1s, S 2s and S 2p peaks (figure 3). XPS of 800 s PIII-treated PES has an additional N 1s peak (figure 3*e*) formed owing to radical reactions of PES macromolecules with bombarding nitrogen ions and atmospheric nitrogen. The interpretation of the peaks is shown in electronic supplementary material, table S2.

The C 1s peak of untreated PES was fitted with a sum of two Lorenz functions with the maximums at 285.0 eV (C–C, C–H, C=C and C–S) and 286.7 eV (C–O–C). In

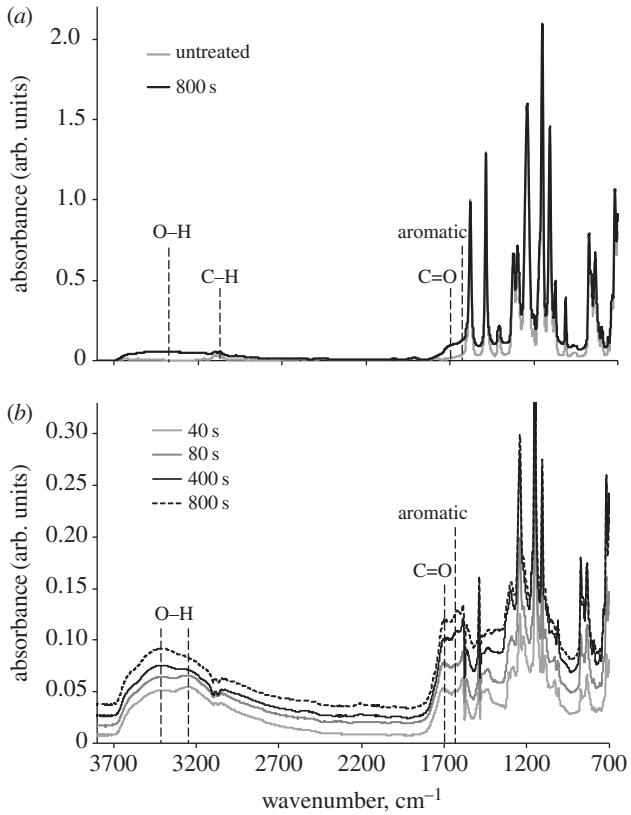

Figure 2. (*a*) FTIR-ATR spectra of untreated and 800 s PIII-treated PES. (*b*) Difference FTIR-ATR spectra of PIII-treated PES after subtraction of the untreated PES spectrum. All spectra were normalized, using the intensity of 1578 cm^{-1} vibration line.

the literature [27–29], the peak at 291.9 eV the C 1s peak is often represented by a sum of at least three peaks corresponding to aromatic moiety (285.0 eV), C–S (285.6 eV) and C–O–C (286.5 eV) groups. We did not separate the peaks of aromatic carbon and C–S groups, because the half width of the peaks used for the fitting is almost three times larger than the difference between the positions of these two peaks.

PIII treatment and post-treatment oxidation result in the formation of a wide range of nitrogen- and oxygen-containing groups. The C 1s peak of 800 s PIII-treated PES was fitted with a sum of five Lorenz functions representing C–O, C=O, C–N, C=N, O–C–O and O–C=O groups (electronic supplementary material, table S2). The O 1s peak of untreated PES consists of two peaks corresponding to $-SO_2-$ (532.0 eV) and C–O–C (533.7) groups. PIII treatment results in the decrease of the intensity of $-SO_2-$ (531.7 eV) and C–O–C (533.8 eV) peaks and the appearance of a new peak at 532.7 eV (C=O). An increased concentration of C=O groups was also observed in the FTIR-ATR spectra of PIII-treated PES (figure 2*b*). The N 1s band of 800 s PIII-treated PES is formed by three components owing to nitrogen in N–C (399.2 eV), N–H (400.4 eV) and $-NH_x^+$ (401.8 eV) groups.

The S 2p peak of untreated PES is represented by a characteristic doublet of $2p_{1/2}$–$2p_{2/3}$ components at about 168.0 eV ($-SO_2-$). After PIII treatment, the intensity of $-SO_2-$ peak significantly decreases and a new intensive peak corresponding to –S– groups appears at about 164.0 eV. The fitting of the S 2p peak of the PIII-treated sample is complicated by a doublet nature of the peak, so the fitting was performed for S 2s peaks. The S 2s peak of untreated PES consists of two peaks at 229.4 eV (–S–, S–H, –SO–) and 232.1 eV ($-SO_2-$). The presence of O–H and S–H groups in untreated PES, arising from polymerization defects, is also observed by FTIR-ATR (electronic supplementary material, figure S1). The vibration lines corresponding to O–H (3640 cm^{-1} and 3550 cm^{-1}) and S–H (2600 cm^{-1}) groups come from post-polymerization end group residuals. PIII treatment results in a sharp decrease of the intensity of the $-SO_2-$ peak (232.2 eV), an increase of the –S– peak (228.0 eV), and the appearance of new two peaks at 226.0 eV (C–S–C) and 230.0 eV (–SO–).

3.5. Wettability

PIII treatment significantly improves wettability of PES (figure 4*a*). The water contact angle decreases from 82° for untreated PES to 39° for 40 s PIII-treated PES (measured two weeks after PIII treatment). The water contact angle of 800 s PIII-treated PES is higher than the water contact angle of 40 s PIII-treated PES. A similar trend was observed for PIII-treated polystyrene [12], polycarbonate [30] and polysulfone [31] when hydrophobic recovery was faster for the samples PIII treated for longer times.

Figure 4*b* shows that the increase of surface free energy of PIII-treated PES is a result of the increase of its polar component. The dispersive part of surface free energy is constant. The increase of the polar part of the surface free energy is observed owing to the high concentration of radicals in the modified surface layer and the formation of highly polar acidic groups, $-SO_2OH$. Two weeks after PIII treatment, the surface free energy of PIII-treated PES has a maximum at 80 s of PIII treatment. Samples treated for longer times show a lower concentration of acidic groups owing to higher levels of carbonization and hence have higher final contact angles.

3.6. Stable, functional tropoelastin coating of polyethersulfone surfaces

Biomolecules such as tropoelastin adhere to untreated, RF plasma-treated or PIII-treated PES at similar levels as detected by the BA4 anti-elastin antibody (figure 5*a*). However, only 15% of the tropoelastin molecules remain bound on untreated PES after hot SDS washing, indicating that the protein is simply physisorbed on the untreated surface. In contrast, majority of tropoelastin molecules are retained on RF plasma-treated (77%) and PIII-treated (57–70%) PES, suggesting stable, covalent protein attachment to these surfaces. These differences are not statistically significant, indicating that the extent of covalent tropoelastin immobilization is similar between RF plasma- and PIII-treated PES, and among surfaces with various PIII exposure times.

Tropoelastin bound on untreated, RF plasma-treated or PIII-treated PES has an exposed C-terminal region as detected by a specific anti-C-terminal peptide antibody (figure 5*b*). This region, which is one of the cell-binding sites within tropoelastin, is accessible when the protein is associated with the PES surface in either physiological (PBS, pH 7.4) or low salt, high pH (PB, pH 11.5) conditions.

Accordingly, tropoelastin-coated PES supports the adhesion of cells such as human dermal fibroblasts

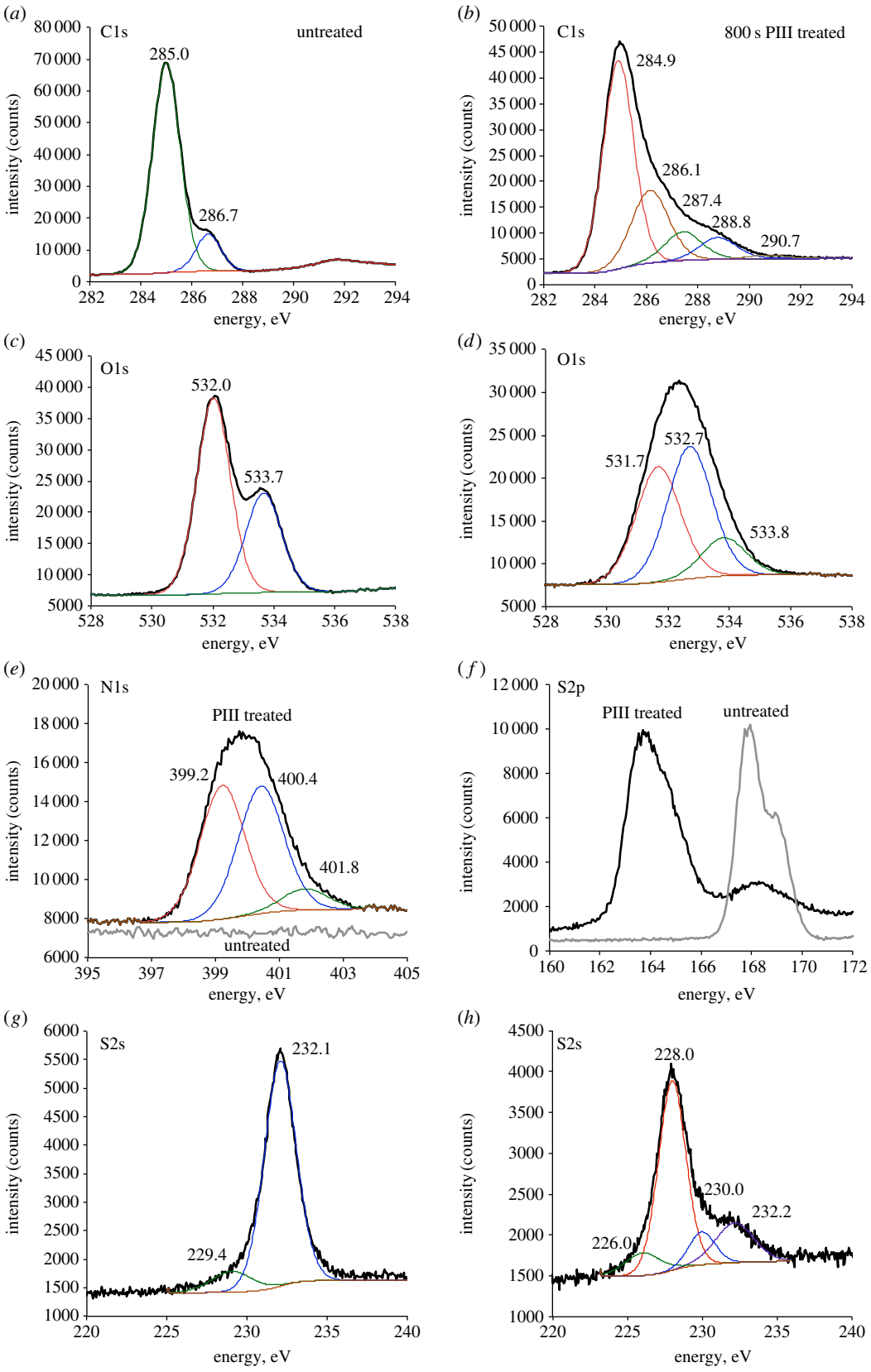

Figure 3. XPS of untreated and PIII-treated PES. C1s peaks of untreated (*a*) and 800 s PIII-treated (*b*) PES. O1s peaks of untreated (*c*) and 800 s PIII-treated (*d*) PES. N1s peaks of untreated and 800 s PIII-treated PES are shown on the same graph (*e*). S2p peaks of untreated and 800 s PIII-treated PES are shown on the same graph (*f*). S2s peaks of untreated (*g*) and 800 s PIII-treated (*h*) PES. C1s, O1s, N1s and S2s peaks were fitted using a sum of Lorenz functions with the positions of peak maximums indicated in the corresponding figures.

(figure 5*c*). Cells do not attach to BSA-blocked PES, but bind well to PES functionalized with tropoelastin prior to BSA blocking. Cell adhesion levels are similar on untreated PES, regardless of protein–surface association conditions, but are higher on PIII-treated PES where tropoelastin was immobilized in a low salt, high pH environment.

3.7. Functionality of tropoelastin-coated polyethersulfone after ethylene oxide sterilization

The ability of biofunctionalized materials to withstand medical-grade sterilization is of paramount importance for translation into clinical use. There is no significant decrease

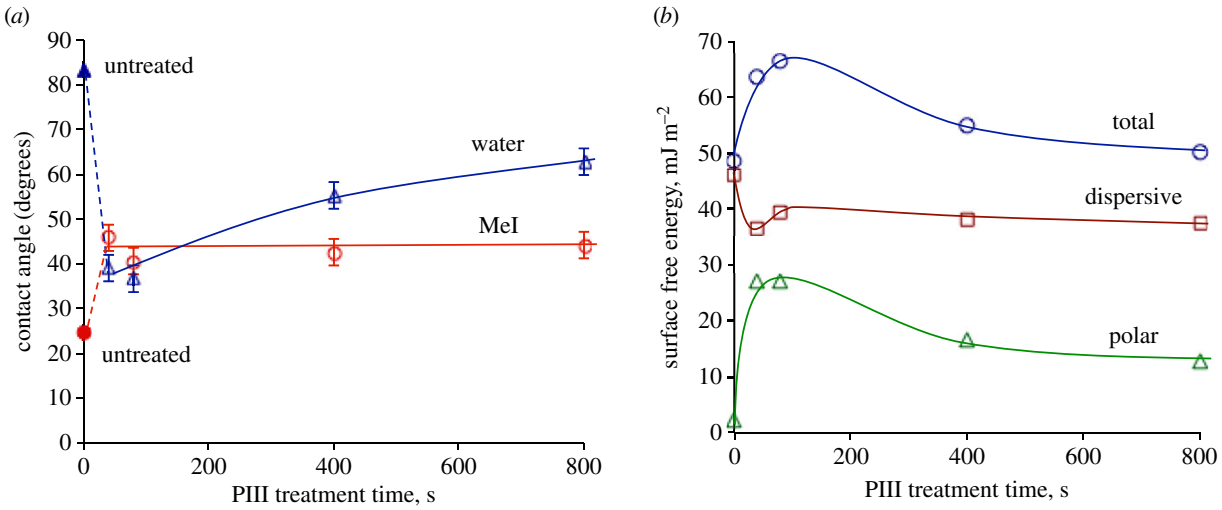

Figure 4. (*a*) Water and diiodomethane (MeI) contact angles of PIII-treated PES depending on time of PIII treatment. (*b*) Surface free energy and its dispersive and polar components for PIII-treated PES as a function of PIII treatment time. The contact angles were measured two weeks after PIII treatment and trend lines were added to guide the eye.

in the total amount of surface-bound tropoelastin detected by an anti-elastin antibody after sterilization with EtO, regardless of whether the protein was associated with the surface at pH 7.4 or pH 11.5 (figure 6*a*,*b*). However, the tropoelastin C-terminus is 39% less accessible on PIII-treated PES than on untreated PES when the protein is bound to the surface at pH 7.4. Moreover, the availability of this region decreases a further 30% on PIII-treated PES, while remaining constant on untreated PES, after EtO sterilization (figure 6*c*). In contrast, the tropoelastin C-terminus is equally accessible on untreated and PIII-treated PES when the protein is coated on the surface at pH 11.5. Furthermore, the extent of C-terminal exposure is maintained after treatment with EtO (figure 6*d*).

The relative accessibility of the tropoelastin C-terminal region is correlated to the level of cell binding activity on the protein-coated surfaces (figure 6*e*,*f*). Surfaces such as untreated PES, where the tropoelastin C-terminus is detected at similarly high levels, regardless of association pH and EtO sterilization, support consistently high levels of fibroblast adhesion. However, cell binding on PIII-treated PES is 60% less than that on untreated PES and further decreases by 33% post-sterilization, when tropoelastin is immobilized to the surface at pH 7.4. In high protein–surface association pH conditions, cell attachment levels on untreated and PIII-treated PES are comparable, and, importantly, are maintained after EtO sterilization.

The ability of tropoelastin to retain functionality after sterilization is a property unique to this protein. Fibronectin adsorbed on untreated PES and kept dry prior to testing is not cell-adhesive even before sterilization, whereas fibronectin immobilized on PIII-treated PES loses 64% of cell binding activity after EtO treatment (figure 6*g*). The loss of fibronectin functionality on untreated PES occurs after sample drying, a prerequisite step to EtO treatment. Fibronectin-coated surfaces stored in hydrated, buffered conditions promote high levels of cell adhesion comparable to tropoelastin-coated surfaces. However, cell attachment on fibronectin-coated surfaces decreases significantly after the samples are dried then rehydrated in PBS, and this decrease is more profound on untreated PES (77%) than on PIII-treated PES (26%) (figure 6*h*). In contrast, the cell attachment capability of tropoelastin-coated PES is completely preserved after sample drying and rehydration.

3.8. Fibroblast morphology and proliferation on sterilized tropoelastin-functionalized polyethersulfone

Tropoelastin coating of PES not only supports high levels of cell adhesion to the surface, but also actively promotes cell proliferation (figure 7). Human dermal fibroblasts show significantly increased numbers on EtO-sterilized tropoelastin-coated surfaces from three days post-seeding. After a 7 day proliferation period, cell numbers on tropoelastin-coated, BSA-blocked untreated PES and PIII-treated PES are 2.2-fold and 1.4-fold higher, respectively, compared with BSA-blocked surfaces. Furthermore, the pH at which tropoelastin is bound to the PES surface does not affect the extent of cell proliferation. The levels of cell proliferation on tropoelastin-functionalized PES are comparable to those achieved on bare and fibronectin-coated tissue culture plastic.

Fibroblasts cultured on bare and tropoelastin-coated untreated and PIII-treated PES surfaces display typical elongated spindle-like morphology throughout the 7 day proliferative period, similar to cells grown on tissue culture plastic controls (figure 8). Representative images of these cells also qualitatively illustrate increased numbers on the PIII and tropoelastin-functionalized PES compared with bare untreated PES, and at levels similar to tissue culture plastic, at 7 days post-seeding.

4. Discussion

PES is one of the most widely used polymers in the biomedical field owing to its mechanical, thermal, oxidative and hydrolytic stability [1]. However, bare PES suffers from inadequate biocompatibility [32,33], which may be aggravated by the non-specific adhesion and subsequent denaturation of biomolecules [34] that hinder target cell interactions or actively elicit an inflammatory or foreign body

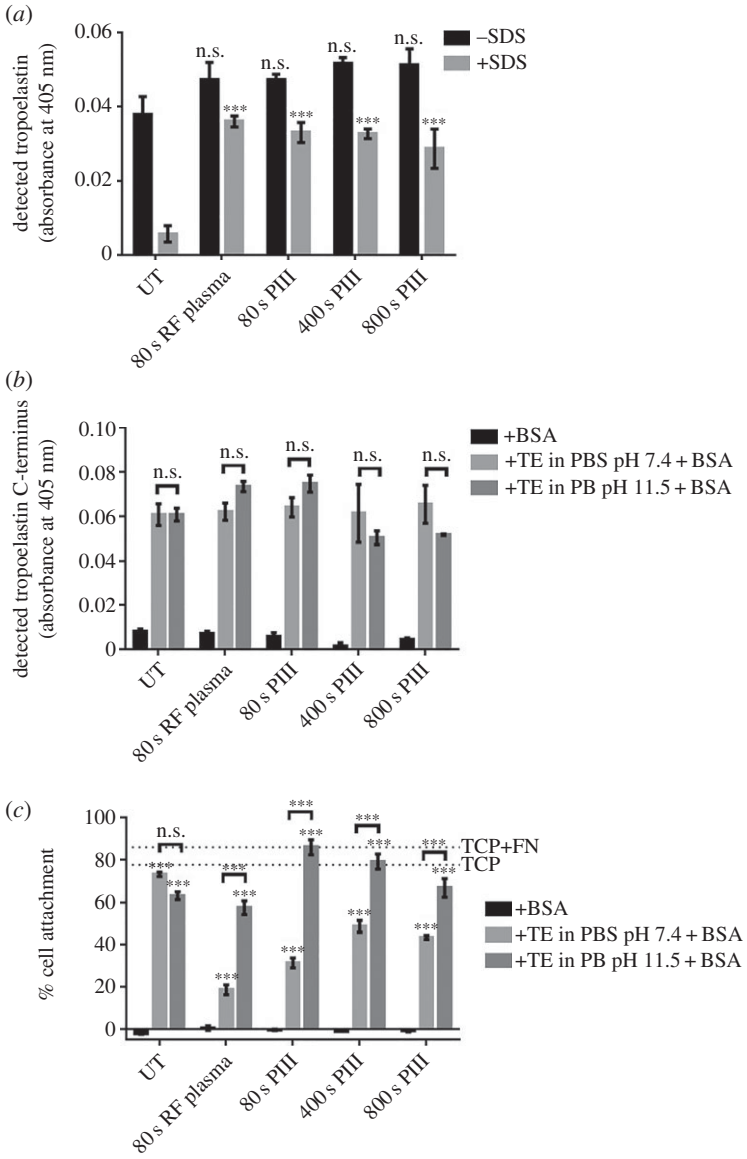

Figure 5. (*a*) Covalent immobilization of tropoelastin (in PBS, pH 7.4) on RF plasma- and PIII-treated PES in contrast to physisorption on untreated PES. Levels of surface-bound tropoelastin on RF plasma- and PIII-treated PES were compared to those on untreated PES. (*b*) Accessibility of the tropoelastin C-terminal region in different tropoelastin (TE)–surface association conditions. All samples were BSA-blocked after protein adhesion. (*c*) Human dermal fibroblast attachment on untreated, RF plasma- and PIII-treated PES with or without tropoelastin (TE). Tropoelastin was coated on the surfaces in different pH and salt conditions, but cell attachment was performed in physiologically relevant conditions. Cell binding was compared between tropoelastin-coated and BSA-coated surfaces, and between tropoelastin-coated surfaces with different protein–surface association conditions.

response to the polymeric material [17,34]. The *in vitro* or *in vivo* biocompatibility of PES can be improved by surface modification with a stable, bioactive protein layer that resists molecular fouling and modulates specific cell responses. The protein immobilization process is ideally simple, rapid, effective, irreversible and non-reliant on potentially cytotoxic chemical linkers.

Protein adsorption depends on the material's surface chemistry, surface charge, topography and wettability, as well as the concentration, ionic strength, pH and temperature of the protein solution [20–22]. Previous studies have shown that PIII treatment has a negligibly low effect on the average roughness of water insoluble polymers, but dramatically changes the polymer surface chemistry and wettability [30].

Bombardment with 20 keV nitrogen ions breaks bonds in polymer macromolecules, displaces atoms and electrons, excites phonons and produces a high concentration of radicals in the modified surface layer [35] that results in a sharp increase in the polar part of surface free energy and significantly improves surface wettability. The decay of the radicals over time after PIII treatment leads to a decrease in the polar part of the surface free energy and hydrophobic recovery. As shown with PIII-treated polystyrene, the rate constants of radical decay have similar values to the rate constants of hydrophobic recovery [12]. Even after hydrophobic recovery, the water contact angle of PIII-treated PES does not reach the value measured for untreated PES. This increased wettability underpins the enhanced bioactivity of surface-immobilized tropoelastin in stimulating fibroblast proliferation (figure 8).

Radicals created by plasma treatment in the subsurface of the polymer are believed to be responsible for the irreversible attachment of protein [17]. The majority of the tropoelastin layer on RF plasma and PIII-treated PES is resistant to hot SDS washing. In contrast, protein molecules that are only physically adsorbed to the surface, such as those on untreated PES, are completely removed. The efficacy of plasma surface modification is such that even a brief (80 s) exposure of PES to RF plasma or PIII generates maximal covalent tropoelastin binding

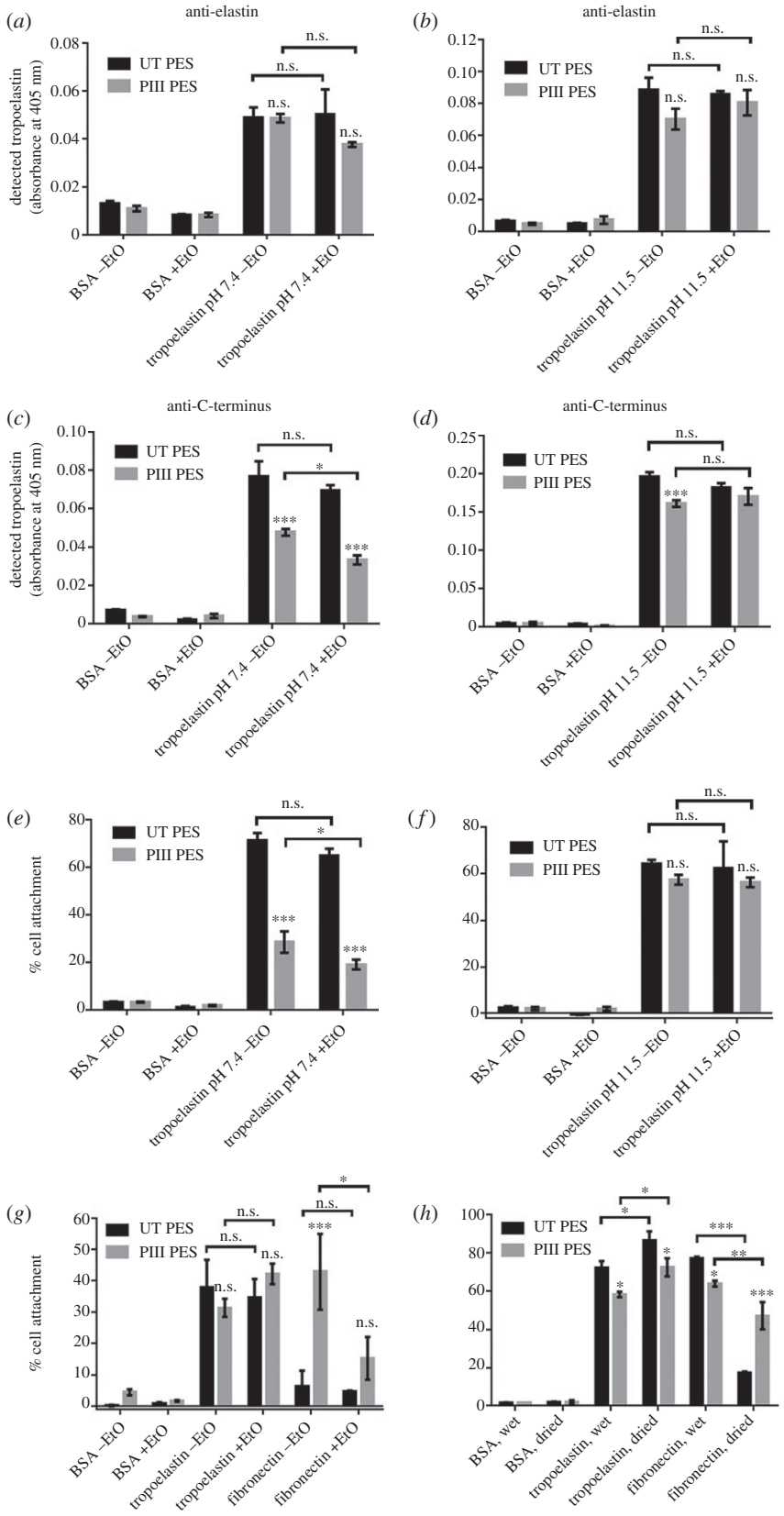

Figure 6. (*a*,*b*) Surface-bound tropoelastin before and after EtO sterilization as detected by the anti-elastin antibody. Tropoelastin was associated to untreated and PIII-treated (400 s) PES at pH (*a*) 7.4 or (*b*) 11.5. (*c*,*d*) Accessibility of the tropoelastin C-terminal region before and after EtO sterilization as detected by a C-terminal peptide antibody. Tropoelastin was associated to the surface at pH (*c*) 7.4 or (*d*) 11.5. (*e*,*f*) Cell attachment to unsterilized and EtO-sterilized tropoelastin-coated samples, in which tropoelastin was associated to the surface at pH (*e*) 7.4 or (*f*) 11.5. (*g*) Cell binding to unsterilized and EtO-sterilized tropoelastin- or fibronectin-coated PES. Tropoelastin was coated on the surface at pH 11.5 while fibronectin was adhered at pH 7.4. (*h*) Cell adhesion to tropoelastin- or fibronectin-coated samples which were kept in PBS or dried prior to the assay. All protein-coated samples were blocked with BSA before cell seeding.

to the surface. This stable linkage minimizes dynamic exchange of the surface-bound tropoelastin with non-specific molecules within a complex heterogeneous cellular environment [36].

A high concentration of radicals was detected in PIII-treated PES using ESR spectroscopy even a month after the PIII treatment (figure 1*c*). These long-living radicals can

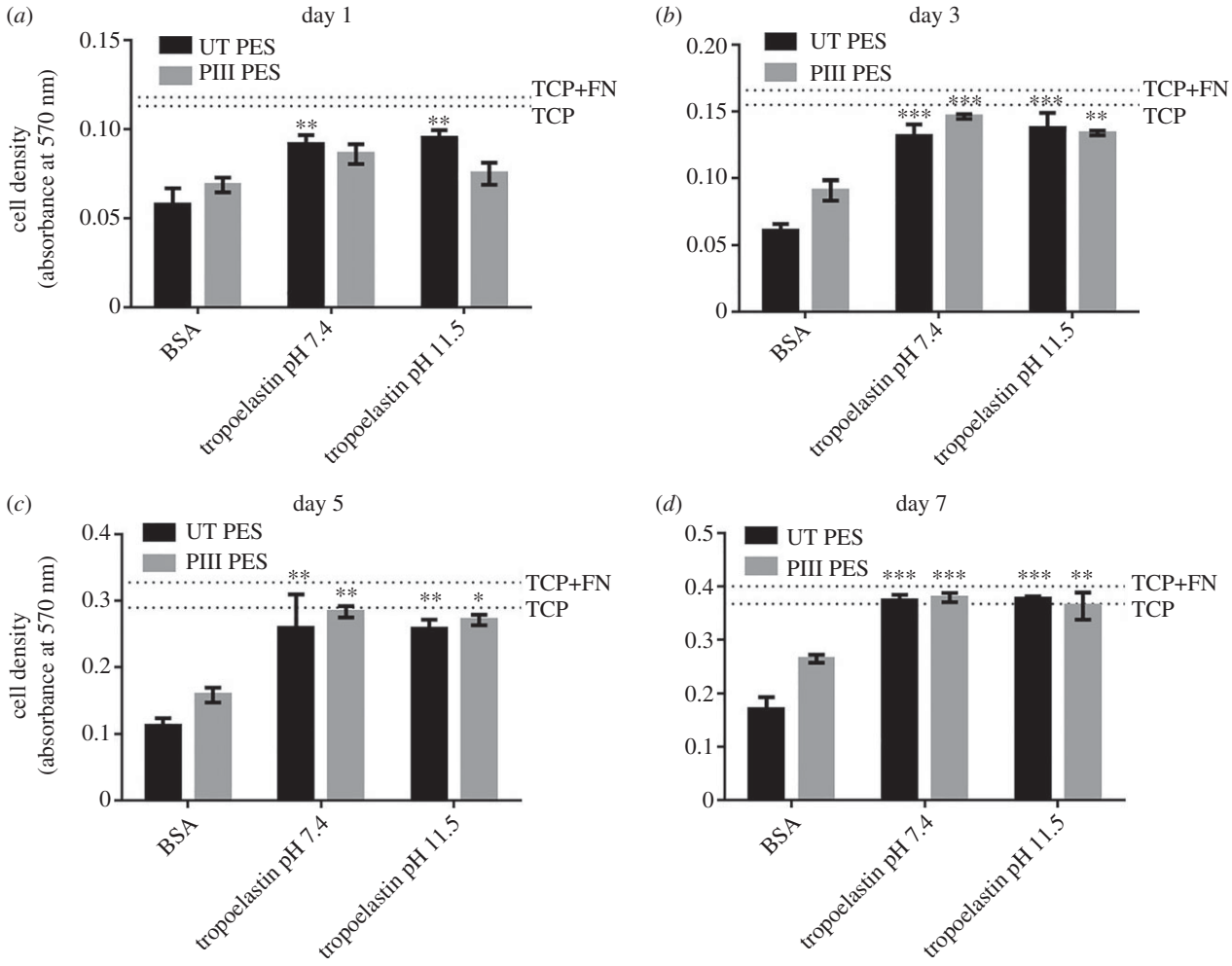

Figure 7. Proliferation of human dermal fibroblasts on EtO-sterilized, untreated and 400 s PIII-treated PES with and without tropoelastin coating. Cell abundance was measured at (*a*) 1, (*b*) 3, (*c*) 5 and (*d*) 7 days post-seeding and compared between the BSA-blocked and tropoelastin-coated, BSA-blocked PES surfaces. The extent of cell growth on tissue culture plastic (TCP) and fibronectin-coated TCP (TCP + FN) controls at each time point are indicated by broken lines.

migrate to the polymer surface and react with proximate protein molecules, providing the polymer with an extended capability for covalent protein attachment [17]. The long-living radicals are stabilized by conjugated structures formed during PIII treatment. The presence of polycyclic carbon structures in PIII-treated PES is confirmed by transmittance measurements (figure 1*a*). The size and number of these structures increase with increasing ion fluence. After 10^{16} ions cm^{-2} (800 s of PIII treatment), a carbonized layer is formed on the surface of PIII-treated polymer [37,38]. This layer improves the chemical resistance of the polymer [31] and has a low degree of post-treatment oxidation [30].

The concentration of acidic groups formed on the PES surface owing to post-treatment oxidation is lower at 800 s than at 80 s of PIII treatment. After the formation of the carbonized layer, SO_2OH groups appear predominantly in the cross-linked layer beneath the carbonized layer owing to a high level of dehydrogenation of the carbonized layer [31].

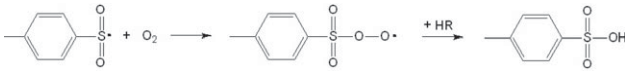

As the high concentration of acidic groups on the surface of PIII-treated PES can affect tropoelastin orientation, the activity of tropoelastin was characterized when it was adhered to untreated and PIII-treated PES in physiologically relevant salt and pH conditions, or in low salt and high pH conditions. In both cases, fibroblast attachment to tropoelastin-coated untreated PES was similar independent of the initial protein–surface association parameters. However, cell binding was significantly higher on tropoelastin-coated PIII-treated PES when the protein was bound to the surface in low salt and high pH conditions. The cell-adhesive tropoelastin C-terminus contains a GRKRK sequence [39] that is positively charged in physiological conditions, which may electrostatically interact with the negatively charged PIII-treated surface and affect its accessibility for functional interactions [9]. In low salt and high pH, the tropoelastin C-terminus is uncharged, which may reduce its surface attraction for maximal availability. This functional protein conformation is maintained when salt and pH conditions are returned to physiological levels during cell binding, owing to covalent stabilization on the PIII-treated surface. In contrast, salt and pH conditions do not significantly affect the orientation of the tropoelastin C-terminus on untreated PES, as electrostatic interactions are not expected to dominate protein adsorption to the more hydrophobic bare PES.

The susceptibility of bare PES materials to biomolecular fouling is demonstrated by the absence of cell adhesion to BSA-blocked untreated or PIII-treated surfaces. On this basis, an important additional benefit of tropoelastin-activated

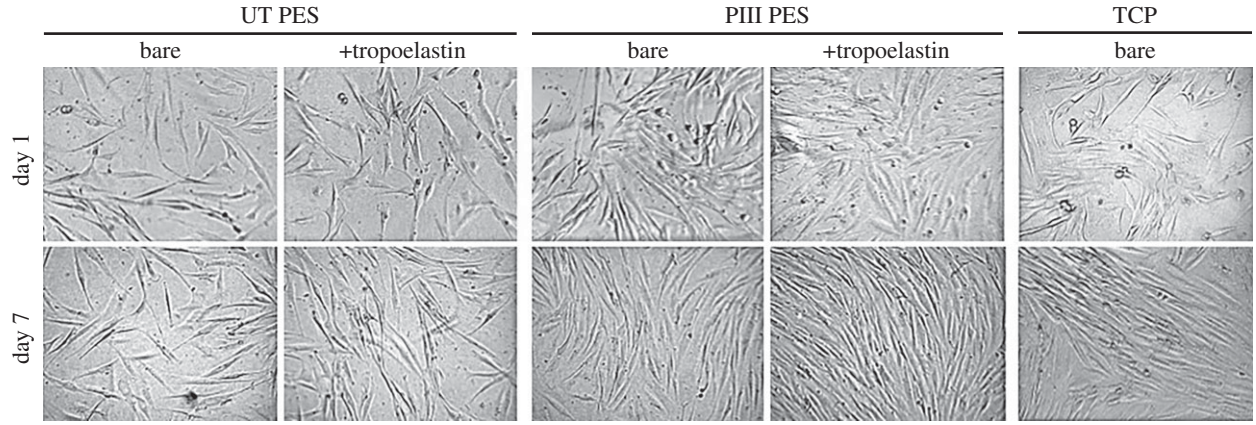

Figure 8. Representative light microscope images of human dermal fibroblasts on bare or tropoelastin-coated, BSA-blocked untreated and 400 s PIII-treated PES, and on tissue culture plastic (TCP) controls, taken at 1 and 7 days post-seeding.

PES is its resistance to subsequent non-specific protein deposition, as evidenced by functional cell binding to surfaces that had been in contact with the BSA blocker after tropoelastin immobilization. The extent of cell attachment to tropoelastin-coated, BSA-blocked untreated or PIII-treated PES was comparable to tissue culture plastic controls.

The ability of the surface-grafted tropoelastin layer to withstand medical-grade sterilization is critical for translation into clinical use. Tropoelastin immobilized on metals treated with plasma-activated coating has previously been shown to resist degradation after steam autoclaving and gamma-ray irradiation dosages up to 40 kGy [11]. However, some polymer substrates are thermally or radiation unstable and can exhibit a decrease in mechanical properties after exposure [40–42]. Such polymers may be subjected to alternative sterilization methods such as exposure to EtO gas. EtO is a highly reactive and highly diffusible agent that inactivates microorganisms by alkylating, and consequently denaturing, essential nucleic acid and protein cellular constituents [43]. As a result, EtO sterilization is overwhelmingly unsuitable for materials with biological components, not only owing to a reduction of bioactivity, but also owing to cytotoxicity risks of residual EtO [44–46]. Remarkably, the amount, orientation and activity of PES-bound tropoelastin are fully retained after EtO sterilization. Accordingly, PIII-treated, tropoelastin-coated surfaces are functional after EtO sterilization, as demonstrated by high levels of cell adhesion, if the protein was bound to the surface in the active conformation with low salt, high pH conditions. While the exact mechanisms of tropoelastin resistance to EtO are unknown, EtO is thought to form adducts mainly with methionine, cysteine and histidine residues [47], which are either absent (i.e. methionine and histidine) or present in very low quantities (i.e. cysteine) in tropoelastin. Furthermore, EtO retention in tropoelastin-coated PES is presumably low, because prolonged pre-leaching of residual EtO into buffer, a necessary step for EtO-sterilized biomaterials [46], was not needed prior to the use of these samples in cell assays.

The ability of surface-immobilized tropoelastin to withstand EtO sterilization is a property unique to this protein. Untreated and PIII-treated PES coated with fibronectin, another cell-adhesive ECM protein, exhibited significant loss of cell binding activity post-sterilization. The decrease in fibronectin bioactivity on PIII-treated PES occurred to the greatest extent after exposure to EtO, whereas that on untreated PES occurred primarily after sample drying prior to EtO exposure. We postulate that majority of the adsorbed fibronectin molecules on untreated PES are lost or irreversibly denatured during the drying process, while those on PIII-treated PES are retained and stabilized due to covalent linkages to the surface. However, treatment with EtO chemically denatures the immobilized fibronectin, possibly through the alkylation of methionine, histidine and cysteine residues abundant throughout the protein sequence, leading to the loss of protein functionality. In contrast, tropoelastin possesses a highly flexible structure [48] that may protect against aberrant folding even on untreated PES. This property, coupled with its resistance to EtO reactivity, allows its functional persistence on PES surfaces during the drying and EtO exposure stages of the sterilization process.

Tropoelastin-coated PES surfaces not only support fibroblast cell adhesion but also promote significantly increased levels of proliferation compared with bare and BSA-blocked untreated or PIII-treated PES, without visibly altering the typical spindle-shaped fibroblast morphology [49]. Tropoelastin modulation of cell activity is thought to be mediated through integrin [5,39] and glycosaminoglycan [6] cell receptor binding sites within the central and C-terminal regions of the molecule. The cytocompatibility and signalling capacity of tropoelastin are expected to be translatable to a range of cell types including vascular endothelial cells, osteoblasts and haemopoietic stem cells [11,50–52]. This functional versatility enables utilization of PIII treatment and tropoelastin cloaking in the functionalization of PES surfaces for diverse research and medical applications.

5. Conclusion

A sequential approach of PIII treatment followed by tropoelastin coating can be used to functionally modify two-dimensional polymer surfaces such as PES, resulting in a sterilizable, stable, hydrophilic, low-fouling, biomimetic and bioactive material for cellular interactions. Two weeks after treatment, 80 s PIII-treated PES surfaces have the highest surface free energy and the highest concentration of acidic groups owing to radical reactions with atmospheric oxygen. Following irreversible tropoelastin immobilization in low salt and high pH conditions, the functionalized surfaces

fully preserve bioactivity after EtO sterilization, evidenced by high levels of fibroblast adhesion and proliferation and a maintenance of cell morphology.

Authors' contributions. G.C.Y. performed and analysed the biochemical and cell experiments, and co-wrote the manuscript. A.K. performed and analysed the physical characterization experiments. E.K. co-wrote the manuscript. A.S.W. and M.M.B. provided feedback at all stages of experimentation, data analysis and manuscript writing. All authors gave final approval for publication.

Competing interests. A.S.W. is the Scientific Founder of Elastagen Pty Ltd.

Funding. This work was supported by the Cooperative Research Centre for Cell Therapy Manufacturing.

References

1. Irfan M, Idris A. 2015 Overview of PES biocompatible/hemodialysis membranes: PES–blood interactions and modification techniques. *Mater. Sci. Eng*. **C56**, 574–592. (doi:10.1016/j.msec.2015.06.035)
2. Chen S, Li L, Zhao C, Zheng J. 2010 Surface hydration: principles and applications toward low-fouling/nonfouling biomaterials. *Polymer* **51**, 5283–5293. (doi:10.1016/j.polymer.2010.08.022)
3. Yin G, Janson JC, Liu Z. 2000 Characterization of protein adsorption on membrane surface by enzyme linked immunoassay. *J. Membr. Sci.* **178**, 99–105. (doi:10.1016/S0376-7388(00)00484-1)
4. Mithieux SM, Wise SG, Weiss AS. 2013 Tropoelastin: a multifaceted naturally smart material. *Adv. Drug Deliv. Rev*. **65**, 421–428. (doi:10.1016/j.addr.2012.06.009)
5. Lee P, Bax DV, Bilek MM, Weiss AS. 2014 A novel cell adhesion region in tropoelastin mediates attachment to integrin alphaVbeta5. *J. Biol. Chem*. **289**, 1467–1477. (doi:10.1074/jbc.M113.518381)
6. Broekelmann TJ, Kozel BA, Ishibashi H, Werneck CC, Keeley FW, Zhang L, Mecham RP. 2005 Tropoelastin interacts with cell-surface glycosaminoglycans via its COOH-terminal domain. *J. Biol. Chem*. **280**, 40 939–40 947. (doi:10.1074/jbc.M507309200)
7. Wachi H, Sugitani H, Murata H, Nakazawa J, Mecham RP, Seyama Y. 2004 Tropoelastin inhibits vascular calcification via 67-kDa elastin binding protein in cultured bovine aortic smooth muscle cells. *J. Atheroscler. Thromb*. **11**, 159–166. (doi:10.5551/jat.11.159)
8. Almine JF, Wise SG, Hiob M, Singh NK, Tiwari KK, Vali S, Abbasi T, Weiss AS. 2013 Elastin sequences trigger transient proinflammatory responses by human dermal fibroblasts. *FASEB J*. **27**, 3455–3465. (doi:10.1096/fj.13-231787)
9. Bax DV, Liu SJ, McKenzie DR, Bilek MMM, Weiss AS. 2011 Tropoelastin switch and modulated endothelial cell binding to PTFE. *BioNanoScience* **1**, 123–127. (doi:10.1007/s12668-011-0018-1)
10. Michael P, Wise S, Bilek M, Weiss A, Ng M. 2013 Tropoelastin selectively inhibits smooth muscle cell proliferation. *Heart Lung Circ*. **22**, S52. (doi:10.1016/j.hlc.2013.05.125)
11. Yeo GC, Santos M, Kondyurin A, Liskova J, Weiss AS, Bilek MMM. 2016 Plasma-activated tropoelastin functionalization of zirconium for improved bone cell response. *ACS Biomater. Sci. Eng*. **2**, 662–676. (doi:10.1021/acsbiomaterials.6b00049)
12. Kosobrodova E, Kondyurin A, McKenzie DR, Bilek MMM. 2013 Kinetics of post-treatment structural transformations of nitrogen plasma ion immersion implanted polystyrene. *Nucl. Instrum. Methods Phys. Res. B: Beam Interact. Mater. Atoms* **304**, 57–66. (doi:10.1016/j.nimb.2013.03.038)
13. Han S, Lee Y, Kim H, Kim G-H, Lee J, Yoon J-H, Kim G. 1997 Polymer surface modification by plasma source ion implantation. *Surf. Coat. Technol*. **93**, 261–264. (doi:10.1016/S0257-8972(97)00057-1)
14. Kondyurin A, Naseri P, Fisher K, McKenzie DR, Bilek MMM. 2009 Mechanisms for surface energy changes observed in plasma immersion ion implanted polyethylene: the roles of free radicals and oxygen-containing groups. *Polym. Degrad. Stab*. **94**, 638–646. (doi:10.1016/j.polymdegradstab.2009.01.004)
15. Kosobrodova EA, Kondyurin AV, Fisher K, Moeller W, McKenzie DR, Bilek MMM. 2012 Free radical kinetics in a plasma immersion ion implanted polystyrene: theory and experiment. *Nucl. Instrum. Methods Phys. Res. B: Beam Interact. Mater. Atoms* **280**, 26–35. (doi:10.1016/j.nimb.2012.02.028)
16. Wakelin EA, Kondyurin AV, Wise SG, McKenzie DR, Davies MJ, Bilek MMM. 2015 Bio-activation of polyether ether ketone using plasma immersion ion implantation: a kinetic model. *Plasma Process. Polym*. **12**, 180–193. (doi:10.1002/ppap.201400149)
17. Bilek MMM *et al.* 2011 Free radical functionalization of surfaces to prevent adverse responses to biomedical devices. *Proc. Natl Acad. Sci. USA* **108**, 14 405–14 410. (doi:10.1073/pnas.1103277108)
18. Gan BK, Kondyurin A, Bilek MMM. 2007 Comparison of protein surface attachment on untreated and plasma immersion ion implantation treated polystyrene: protein islands and carpet. *Langmuir* **23**, 2741–2746. (doi:10.1021/la062722v)
19. Kosobrodova E, Jones RT, Kondyurin A, Chrzanowski W, Pigram PJ, McKenzie DR, Bilek MMM. 2015 Orientation and conformation of anti-CD34 antibody immobilised on untreated and plasma treated polycarbonate. *Acta Biomater*. **19**, 128–137. (doi:10.1016/j.actbio.2015.02.027)
20. Rabe M, Verdes D, Seeger S. 2011 Understanding protein adsorption phenomena at solid surfaces. *Adv. Colloid Interface Sci*. **162**, 87–106. (doi:10.1016/j.cis.2010.12.007)
21. Whittle J, Bullett N, Short R, Douglas I, Hollander A, Davies J. 2002 Absorption of vitronectin, collagen and immunoglobulin-G to plasma polymer surface by enzyme linked immunosorbent assay (ELISA). *J. Mater. Chem*. **12**, 2726–2732. (doi:10.1039/b201471h)
22. Chen S, Liu L, Zhou J, Jiang S. 2003 Controlling antibody orientation on charged self-assembled monolayers. *Langmuir* **19**, 2859–2864. (doi:10.1021/la026498v)
23. Kondyurin A, Bilek MMM. 2008 *Ion beam treatment of polymers. Application aspects from medicine to space*. Amsterdam, The Netherlands: Elsevier.
24. Freidel R, Orchin M. 1951 *Ultraviolet spectra of aromatic compounds*. New York, NY: Wiley.
25. Ruiterkamp R, Halasinski T, Salama F, Foing B, Allamandola L, Schmidt W, Ehrenfreund P. 2002 Spectroscopy of large PAHs. *Astron. Astrophys*. **390**, 1153–1170. (doi:10.1051/0004-6361:20020478)
26. Biersack JP, Ziegler JF. 1982 The stopping and range of ions in solids. In *Ion implantation techniques* (eds H Ryssel, H Glawischnig). Springer Series in Electrophysics, vol. 10, pp. 122–156. Berlin, Germany: Springer. (doi:10.1007/978-3-642-68779-2_5)
27. Bormashenko E, Grynyov R, Bormashenko Y, Drori E. 2012 Cold radiofrequency plasma treatment modifies wettability and germination speed of plant seeds. *Sci. Rep*. **2**, 741. (doi:10.1038/srep00741)
28. Wavhal DS, Fisher ER. 2005 Modification of polysulfone ultrafiltration membranes by CO_2 plasma treatment. *Desalination* **172**, 189–205. (doi:10.1016/j.desal.2004.06.201)
29. Zhu L-P, Zhu B-K, Xu L, Feng Y-X, Liu F, Xu Y-Y. 2007 Corona-induced graft polymerization for surface modification of porous polyethersulfone membranes. *Appl. Surf. Sci*. **253**, 6052–6059. (doi:10.1016/j.apsusc.2007.01.004)
30. Kosobrodova E, Kondyurin A, Chrzanowski W, McCulloch DG, McKenzie DR, Bilek MMM. 2014 Optical properties and oxidation of carbonized and cross-linked structures formed in polycarbonate by plasma immersion ion implantation. *Nucl. Instrum. Methods Phys. Res. B: Beam Interact. Mater. Atoms* **329**, 52–63. (doi:10.1016/j.nimb.2014.03.010)
31. Kosobrodova E, Kondyurin A, Chrzanowski W, McKenzie DR, Bilek MMM. 2016 Plasma immersion ion implantation of a two-phase blend of polysulfone and polyvinylpyrrolidone. *Mater. Des*. **97**, 381–391. (doi:10.1016/j.matdes.2016.02.124)
32. Peppas NA, Langer R. 1994 New challenges in biomaterials. *Science* **263**, 1715–1720. (doi:10.1126/science.8134835)
33. Ran F, Nie S, Zhao W, Li J, Su B, Sun S, Zhao C. 2011 Biocompatibility of modified polyethersulfone

membranes by blending an amphiphilic triblock copolymer of poly(vinyl pyrrolidone)–b-poly(methyl methacrylate)–b-poly(vinyl pyrrolidone). *Acta Biomater*. **7**, 3370–3381. (doi:10.1016/j.actbio.2011.05.026)

34. Kochkodan V, Johnson DJ, Hilal N. 2014 Polymeric membranes: surface modification for minimizing (bio)colloidal fouling. *Adv. Colloid Interface Sci*. **206**, 116–140. (doi:10.1016/j.cis.2013.05.005)
35. Fink D. 2004 *Fundamentals of ion-irradiated polymers*. Berlin, Germany: Springer.
36. Vroman L, Adams AL. 1969 Findings with the recording ellipsometer suggesting rapid exchange of specific plasma proteins at liquid/solid interfaces. *Surf. Sci*. **16**, 438–446. (doi:10.1016/0039-6028(69)90037-5)
37. Marletta G, Catalano SM, Pignataro S. 1990 Chemical reactions induced in polymers by keV ions, electrons and photons. *Surf. Interface Anal*. **16**, 407–411. (doi:10.1002/sia.740160185)
38. Popok V. 2012 Ion implantation of polymers: formation of nanoparticulate materials. *Rev. Adv. Mater. Sci*. **30**, 1–26.
39. Bax DV, Rodgers UR, Bilek MM, Weiss AS. 2009 Cell adhesion to tropoelastin is mediated via the C-terminal GRKRK motif and integrin alphaVbeta3. *J. Biol. Chem*. **284**, 28 616–28 623. (doi:10.1074/jbc.M109.017525)
40. Oliveira LM, Araujo PLB, Araujo ES. 2013 The effect of gamma radiation on mechanical properties of biodegradable polymers poly(3-hydroxybutyrate) and poly(3-hydroxybutyrate-co-3-hydroxyvalerate). *Mater. Res*. **16**, 195–203. (doi:10.1590/S1516-14392012005000173)
41. Fulin P, Pokorny D, Slouf M, Vackova T, Dybal J, Sosna A. 2014 Effect of sterilisation with formaldehyde, gamma irradiation and ethylene oxide on the properties of polyethylene joint replacement components. *Acta Chir. Orthop. Traumatol. Cech*. **81**, 33–39.
42. Madorsky SL, Straus S. 1954 Thermal degradation of polymers as a function of molecular structure. *J. Res. Natl Bureau Standards* **53**, 361–370. (doi:10.6028/jres.053.044)
43. Mendes GCC, Brandão TRS, Silva CLM. 2007 Ethylene oxide sterilization of medical devices: a review. *Am. J. Infect. Control* **35**, 574–581. (doi:10.1016/j.ajic.2006.10.014)
44. Pekkarinen T, Hietalal O, Jamsa T, Jalovaara P. 2005 Gamma irradiation and ethylene oxide in the sterilization of native reindeer bone morphogenetic protein extract. *Scand. J. Surg*. **94**, 67–70. (doi:10.1177/145749690509400116)
45. Grasman JM, O'Brien MP, Ackerman K, Gagnon KA, Wong GM, Pins GD. 2016 The effect of sterilization methods on the structural and chemical properties of fibrin microthread scaffolds. *Macromol. Biosci*. **16**, 836–846. (doi:10.1002/mabi.201500410)
46. Rnjak-Kovacina J, DesRochers TM, Burke KA, Kaplan DL. 2015 The effect of sterilization on silk fibroin biomaterial properties. *Macromol. Biosci*. **15**, 861–874. (doi:10.1002/mabi.201500013)
47. Chen L, Sloey C, Zhang Z, Bondarenko PV, Kim H, Sekhar Kanapuram DR. 2015 Chemical modifications of therapeutic proteins induced by residual ethylene oxide. *J. Pharm. Sci*. **104**, 731–739. (doi:10.1002/jps.24257)
48. Muiznieks LD, Weiss AS. 2007 Flexibility in the solution structure of human tropoelastin. *Biochemistry* **46**, 8196–8205. (doi:10.1021/bi700139k)
49. Fahrenholtz M, Liu H, Kearney D, Wadhwa L, Fraser C, Grande-Allen K. 2014 Characterization of dermal fibroblasts as a cell source for pediatric tissue engineered heart valves. *J. Cardiovasc. Dev. Dis*. **1**, 146. (doi:10.3390/jcdd1020146)
50. Hiob MA, Wise SG, Kondyurin A, Waterhouse A, Bilek MM, Ng MK, Weiss AS. 2013 The use of plasma-activated covalent attachment of early domains of tropoelastin to enhance vascular compatibility of surfaces. *Biomaterials* **34**, 7584–7591. (doi:10.1016/j.biomaterials.2013.06.036)
51. Holst J *et al.* 2010 Substrate elasticity provides mechanical signals for the expansion of hemopoietic stem and progenitor cells. *Nat. Biotechnol*. **28**, 1123–1128. (doi:10.1038/nbt.1687)
52. Yu Y *et al.* 2015 Characterization of endothelial progenitor cell interactions with human tropoelastin. *PLoS ONE* **10**, e0131101. (doi:10.1371/journal.pone.0131101)